

## STUDY ON IONIZATION EFFECTS PRODUCED BY NEUTRON INTERACTION PRODUCTS IN BNCT FIELD\*

M. R. ESKANDARI<sup>1\*\*</sup>, L. REZAEI<sup>1</sup> AND S. MOHAMMADI<sup>2</sup>

<sup>1</sup>Physics Department, Shiraz University, Shiraz 71454, I. R. of Iran  
 eskandari@physics.susc.ac.ir

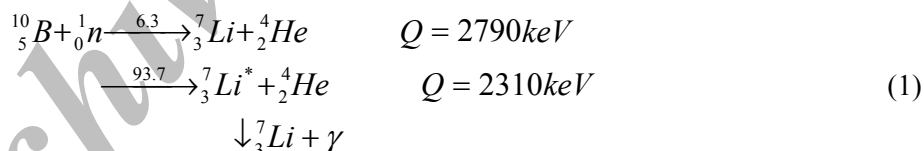
<sup>2</sup>Physics Department, Payam Nour University, Fariman 93914, I. R. of Iran

**Abstract** – The ionization effects of charged particles produced in neutron interactions for Boron Neutron Capture Therapy are considered here using SRIM Monte Carlo Code. The estimated values of these effects in a Plexiglas acrylic phantom are shown to agree well with the available experimental values in high Boron concentration areas. As expected, the ionization effects from lithium and alpha particles are significant. However in the low Boron areas, proton ionization makes an important contribution and their effect on healthy tissue should not be ignored.

**Keywords** – BNCT, ionization effects, Lithium, Alpha, Protons, healthy tissue

### 1. INTRODUCTION

In Boron Neutron Capture Therapy (BNCT) [1], a tumor is irradiated by thermal neutrons [2]. Boron atoms are introduced to the tumor and gather in the cancer cells. Higher thermal neutrons interaction cross-section of Boron causes strong impressive ionization damage to the tumor. Boron-10 thermal neutron capture results in the following nuclear reactions [3]:



The alpha particles and lithium produced have a high LET; they deposit their energy in tissue within ranges of 4.1 and 7.7 $\mu\text{m}$  respectively, which are comparable to a typical cell dimension. The energy deposition depends strongly on spatial deposition of the B-10 nuclei and in concentration in the tumor [4, 5]. In addition to the absorbed dose, due to B-10 neutron capture, many other dose components are present.

Protons are recoil products from the interaction of both fast and epithermal neutrons with H-1 nuclei in  $n + p \rightarrow n' + p'$  interaction.

Alpha particles and Carbon as a recoil product come from the interaction of C-12 nuclei in  ${}^{12}\text{C}(n, n){}^{12}\text{C}$  reaction.

In a BNCT field, interactions between neutron and boron injected into a tumor result in lithium ions and alpha particles. This interaction will take place with high probability as the reaction cross-section is high. The lithium ions and alpha particles produced move into matter and ionize it. In BNCT we study the destructive effects on cancer cells by the motion of these ionizing particles. In addition to the above

\*Received by the editor November 20, 2007 and in final revised form June 1, 2008

\*\*Corresponding author

interaction, neutrons have another interactive mode with atomic nuclei in matter. The interaction of epithermal neutrons with matter in the BNCT field can result in protons, carbon and oxygen ions as products. The charged particles produced move in matter and ionize it, deposit their energy and eventually have remarkable destructive effects. In this research, the ionization effects of all the particles produced in a Plexiglas acrylic phantom are investigated. The unwanted ionization effects are compared with the ionization effects caused by Lithium ions, and alpha particles are considered to be basic ionizing particles in BNCT.

We study charged particle tracks in matter by using SRIM [6]. The precision of a Monte Carlo approach for computing charge particle trajectories in matter depends mainly on the precision of the calculation of the stopping power properties of the matter. A direct calculation of charge particle stopping powers in matter is practically possible using the transport of ions in matter and using the SRIM computer code. It is proved that the SRIM Monte Carlo modeling could adequately predict the dose to tissue in BNCT treatment.

## 2. MATERIAL AND METHOD

To simulate a neutron field and charged particle trajectories, we use a Plexiglas acrylic phantom ( $\rho = 1.17 \text{ g cm}^{-3}$ ,  $C_4H_6O_2$ ) in considering BNCT and simulate charged particles tracks by Monte Carlo computation using the SRIM computer code. This phantom is used so the obtained Monte Carlo calculations can be compared with the available experimental values.

Epithermal neutrons have different modes of interaction with tissue being considered here. Elastic scattering can take place upon interaction with hydrogen, carbon and oxygen nuclei. Elastic scattering cross-sections for these interactions are shown in Fig. 1 [7].

To be able to evaluate the effects of charged particles produced from neutron interactions, the initial energies of particles are needed. In this research, we study the ionization effect by recoiled protons, carbon and oxygen in an elastic scattering of neutron interactions. The ionization effects of alpha and lithium particles which are the product of neutron-Boron interactions are also studied. These results are compared to each other.

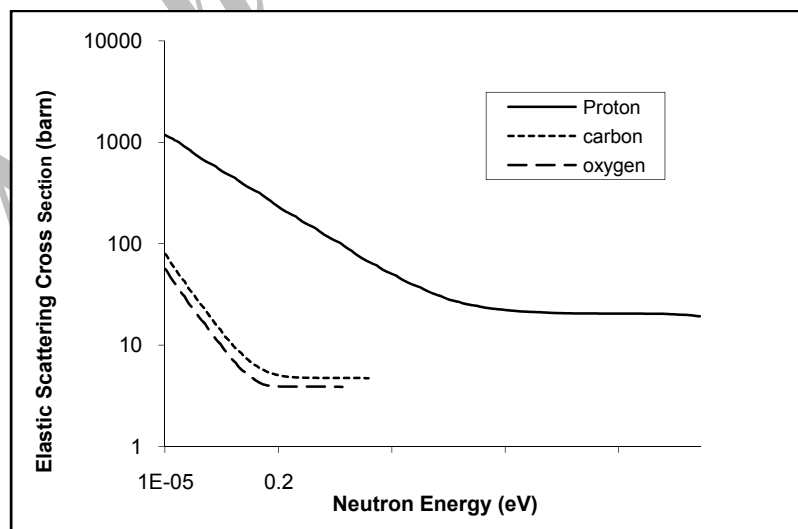


Fig. 1. Elastic scattering cross section variation

Recoiled protons in the elastic scattering of epithermal neutrons by a hydrogen nucleus have the same energy as the incident nucleus; they move in matter and ionize it. These calculations are done by using the

SRIM computer code. Recoiled carbon ions in  $^{12}C(n,n)^{12}C$  and oxygen ions in  $^{16}O(n,n)^{16}O$  elastic interactions have average initial energies of  $2.84keV$  and  $2.215keV$ , respectively.

Furthermore, the thermal neutrons captured by *B-10* result in alpha particles and lithium ions with  $1470keV$  and  $840keV$  initial energies, respectively.

Several useful statistical quantities can be defined to estimate the statistical accuracy of the results obtained by SRIM code. Straggling range, skewness and kurtosis are defined as [8]:

$$\text{Straggling range} \equiv \sigma = \langle (\Delta x)^2 \rangle^{1/2} \quad (2)$$

$$\text{Skewness} \equiv \gamma = \langle \Delta x^3 \rangle / \langle \Delta x^2 \rangle^{3/2} \quad (3)$$

$$\text{Kurtosis} \equiv \beta = \langle \Delta x^4 \rangle / \langle \Delta x^2 \rangle^2 \quad (4)$$

In this way, straggling range is the square root of the variance, which itself is the second moment distribution of the range. The skewness tells whether the peak is skewed towards the surface (negative values) or away from the surface (positive values). Negative skewness indicates that the most probable depth (the peak position) is greater than the mean depth, and positive values indicate the reverse.

Kurtosis indicates the extent of the distribution tails, with a value of 3.0 indicating a Gaussian distribution. Since both the shallow and deep tails contribute, no simple rule indicates what a deviation from 3.0 means for the ion distribution. In general, values from 0 to 3 indicate abbreviated tails, and values above 3 indicate broad tails.

### 3. RESULTS AND DISCUSSION

In the Plexiglas phantom used, the energy loss versus depth due to ionization by alpha particles and lithium ions produced by the capture of thermal neutrons in Boron-10 are shown in Fig. 2. The effects of recoiled particles in this ionization process can be neglected; they are not much in evidence in the Figure. The same curves for carbon and oxygen ions are shown in Figs. 3 and 4, respectively. The effects of recoiled particles in these ionization interactions are comparable to those of the direct ionization effects by carbon and oxygen ions. Furthermore, the energy loss versus depth in Plexiglas due to ionization interactions for protons and recoils are shown in Fig. 5. It can be seen that ionization effects due to the recoiled protons can be neglected.

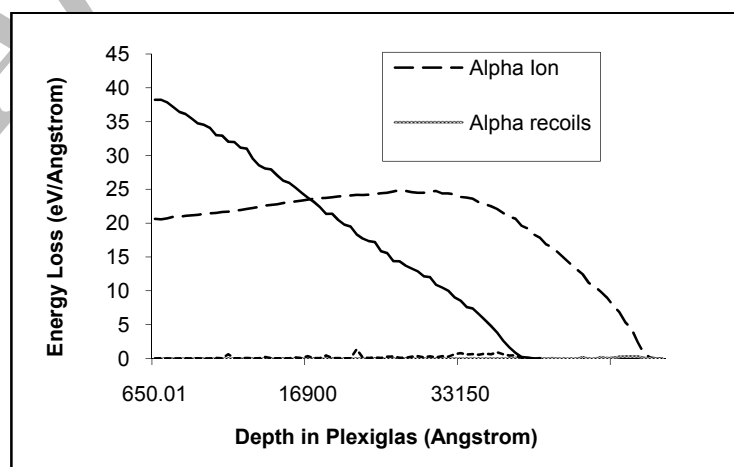


Fig. 2. Lithium ions and alpha energy loss

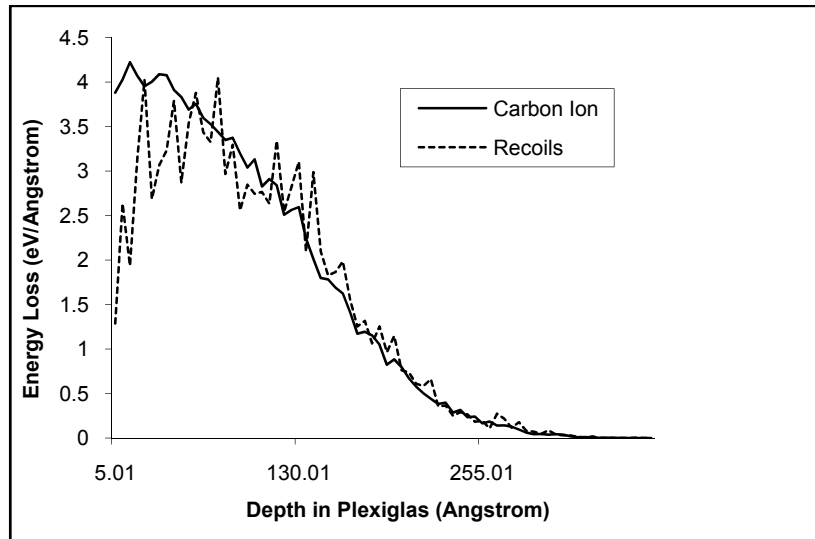


Fig. 3. Carbon ions and recoils energy loss

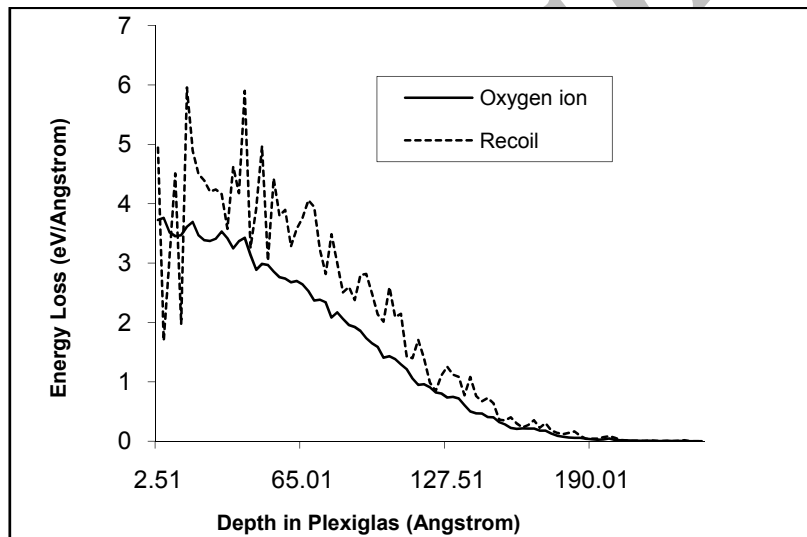


Fig. 4. Oxygen ions and recoils energy loss

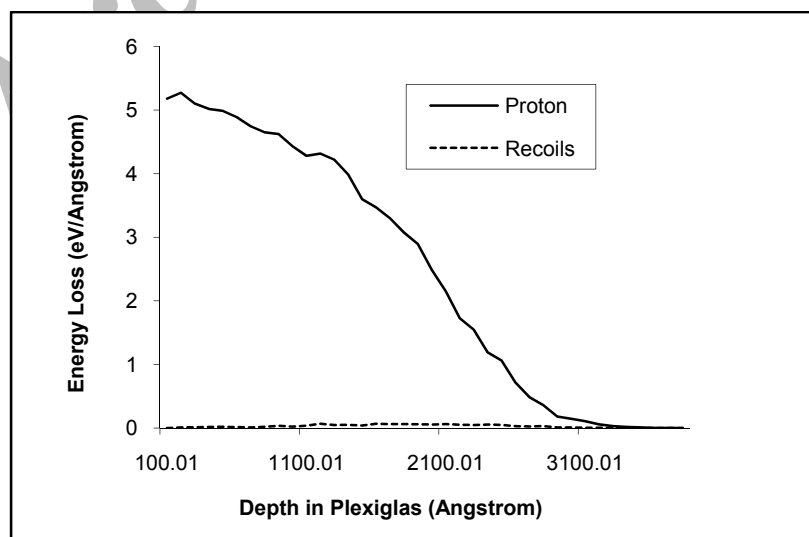


Fig. 5. Proton and recoils energy loss

The calculated ion ranges for the various ions produced are shown in Fig. 6. It can be seen that the alpha particles produced from thermal neutron capture by boron have the largest ion range (from generation to stop location), in comparison to the other particles produced. SRIM results for the calculated ion initial energy, energy loss and defined statistical quantities for various ions are shown in Table 1.

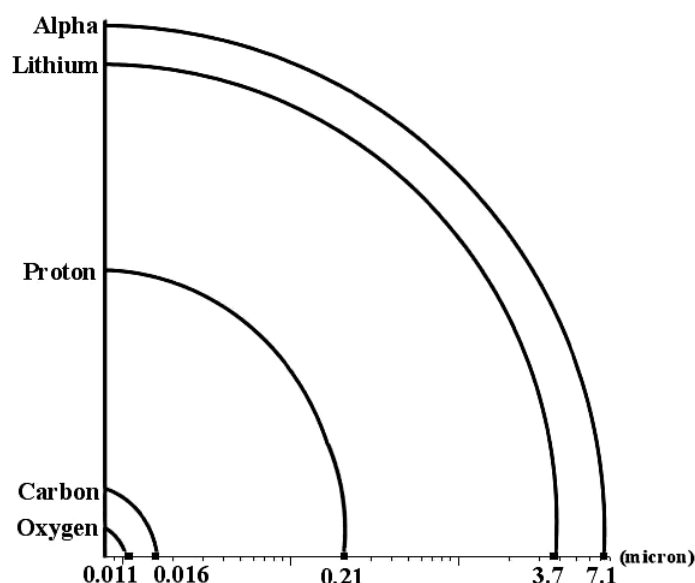


Fig. 6. Comparing radius of spheres

Table 1. SRIM results for energy and statistical quantities

	Proton	Carbon	Oxygen	Alpha	Lithium
Ion Initial Energy (keV)	10	2.84	2.21	1470	840
Energy Loss in Range (keV)	9.172	0.566	0.322	1451	803.3
Recoil Energy Loss (keV)	0.001	0.529	0.426	0.003	0.014
Straggle( $\mu\text{m}$ )	0.050	0.006	0.004	0.164	0.203
Skewness	-0.55	0.10	0.12	-2.69	-3.01
Kurtosis	4.06	2.61	2.59	25.76	30.66

Each alpha particle produced can ionize the matter in a sphere concentrated on the generation location with a radius equal to  $7.120\mu\text{m}$ . From its initial energy ( $1470\text{keV}$ ), it can deposit about 98.6% ( $1450\text{keV}$ ) for ionizing media. Furthermore, it is obvious, as can be seen in Table 1, that oxygen ions have the lowest range in Plexiglas relative to other particles. Every oxygen ion from its initial energy ( $2.21\text{keV}$ ) deposits  $0.332\text{keV}$ , namely 13.57 per cent for direct ionization, and  $0.426\text{keV}$  (18 per cent) for indirect secondary ionization. Ionization energy is saved in a sphere of radius  $0.011\mu\text{m}$  centered on the generation location. The remaining ion energy is spent for increasing thermal vibrations of atoms in media.

In order to be able to compare the straggling range for ions, we define  $\eta$  as

$$\eta = \frac{\sigma}{x} = \frac{\langle(\Delta x)^2\rangle^{1/2}}{x} \quad (5)$$

where  $\eta$  is a criterion for uncertainty concerning the frontier of the spheres. It can be seen (Table 1) that the oxygen and carbon ions have the lowest range of straggling and lithium ions and alpha particles from Boron neutron capture,  $^{10}\text{B}(n,\alpha)^7\text{Li}$ , have the largest straggling. But, the defined  $\eta$  indicates that uncertainty

for lithium ions and alpha particles from  $^{10}B(n,\alpha)^7Li$  is small ( $\sim 10^{-2}$ ) and for other ions becomes larger ( $\sim 10^{-1}$ ).

The skewness values for alpha particles, protons and lithium ions are negative, indicating that their peak is skewed towards the surface. Carbon and oxygen ions have positive skewness, indicating the peak is away from the surface. Therefore, carbon and oxygen ions with high probability will stop before reaching their mean stopping location, while alpha particles, protons and lithium ions will more likely stop after their mean stopping location.

Kurtosis values for carbon and oxygen ions are in the range from 0 to 3 and therefore have abbreviated tails; alpha particles, protons and lithium ions have a kurtosis value above 3 and therefore have broad tails. Kurtosis values for oxygen, carbon and protons indicate a distribution similar to a Gaussian shape.

An experimental evaluation of the beam quality of the clinical BNCT neutron field at the Kyoto University Reactor (KUR) based on a microdosimetric technique was studied by Endo et al. [8]. It was shown that the estimated relative contributions of the neutron dose on proton, alpha particles and carbon ions are 0.9, 0.07 and 0.03, respectively. In this evaluation, the effects of oxygen and lithium ions were not considered.

In the mentioned experimental evaluation, a Tissue Equivalent Proportional Counter (TEPC) and a Carbon Walled Proportional Counter (CWPC) were used for measurements and the results obtained compared. The TEPC and CWPC were filled by a methane-based tissue equivalent and  $CO_2$  gases respectively, at a certain pressure [8].

As CWPC does not contain hydrogen neither in the wall nor in filling gas, the recoiled carbons from elastic scattering produced in tissue can be simulated.

In order to be able to compare the experimental results to our calculated values using SRIM, the percentage of ionization effects by protons, carbon ions and alpha are calculated and given in Table 2. It can be seen that there is a good agreement for protons, but the relative contribution to neutron dose from alpha particles and carbon ions in SRIM calculations are equal.

Table 2. Per cent of ionization effects due to carbon, proton and alpha

	Carbon	Proton	Alpha
Our work	0.055	0.89	0.055
Reference (8)	0.03	0.9	0.07

It is also obvious that ionization effects due to the other particles are insignificant when compared with the effects due to lithium ions and alpha particles. Because of the low concentration of boron in matter as compared with oxygen, hydrogen and carbon, clearly the probability of alpha or lithium production is very small in comparison to protons and recoiled oxygen and carbon atoms. But in fact, the ionization from these particles can have serious effects and damage in the amount of dose absorbed. For example, in a typical experiment, if the boron concentration is considered to be 2000 ppm [4], and we assume the probability of interaction is proportional to particle concentration and neutron interaction cross section ( $\Sigma = N\sigma$ ). In  $10keV$  [7], the calculated percent of ionization effects for these particles is shown in Table 3.

Table 3. Percent of ionization effects due to all charged particles considering particle concentrations and cross sections

Carbon	Proton	Oxygen	Lithium	Alpha
11.17	51.31	4.14	11.89	21.49

It can be seen that the ionization effects depend strongly on protons and so the dose amount needs to be kept low. Furthermore, the ionization effects due to carbon and oxygen ions are not ignorable. In BNCT, we can control the boron concentration in a tumor relative to that in healthy tissue, and therefore we can increase the absorption dose in the tumor relative to healthy tissue, but we should not ignore the effect of protons on healthy tissue.

#### 4. CONCLUSIONS

Our analysis can be summarized briefly as follows:

For the protons, carbon ions, alpha particles, lithium and oxygen ions produced in Boron Neutron Capture Therapy as products from reactions or their recoils, their range and other important statistical parameters were calculated using the SRIM Monte Carlo code. The ionization effects due to these particles were estimated in a Plexiglas acrylic phantom and compared with the available experimental values, showing good agreement. It is also shown that ionization effects due to the recoiled charged particles compared to the effects due to lithium ions and alpha particles are insignificant. Having considered the Boron concentration and relevant neutron beam cross-sections, it is shown that the ionization effect of protons on the healthy tissues is more than the other by-products and should not be ignored. Finally, it is proved that the used SRIM Monte Carlo modeling is adequate to predict the dose to tissue in BNCT treatment.

#### REFERENCES

1. Barth, R. F., Soloway, A. H. & Fairchild, R. G. (1990). Boron Neutron Capture Therapy of Cancer. *Cancer Research*, 50.
2. Eskandari, M. R., et al. (2006). Production of epithermal neutron beam of  $^{238}\text{PuBe}$  neutron source for Boron Neutron Capture Therapy, *Symposium on Radiation Measurement and Applications*, Michigan, USA, Ann Arbor.
3. Knoll, G. F. (2000). *Radiation Detection and Measurement*, 3<sup>rd</sup> ed., New York, Wiley Inc.
4. Daniel, C. M., Xin, L. & Charles, S. (2005). Pharmacothermodynamics of deuterium-induced oedema in living rat brain via  $^1\text{H}_2\text{O}$  MRI: implications for boron neutron capture therapy of malignant brain, tumours, *Phys. Med. Biol.* 50.
5. Tanaka, K., Kobayashi, T., Bengua, G., Nakagawa, Y., Endo, S. & Hoshi, M. (2005). Characteristics of boron-dose enhancer dependent on dose protocol and  $^{10}\text{B}$  concentration for BNCT using near-threshold  $^7\text{Li}(p,n)^7\text{Be}$  direct neutrons. *Phys. Med. Biol.* 50.
6. Ziegler, J. F. & Biersack, J. P. (2003). The stopping and range of ions in matter. *SRIM*, 26.
7. Neutron Cross Section Lab., available in <http://www.nea.fr/janis>.
8. Endo, S., Onizuka, Y., Ishikawa, M., Takada, M., Sakurai, Y., Kobayashi, T., Tanaka, K., Hoshi, M. & Shizuma, K. (2004). Microdosimetry of neutron field for boron neutron capture therapy at Kyoto university reactor. *Radiation Protection Dosimetry*, 110.